Journal of Cranio-Maxillo-Facial Surgery 45 (2017) 1387–1393

Contents lists available at ScienceDirect

Journal of Cranio-Maxillo-Facial Surgery

journal homepage: www.jcmfs.com

Cerebrospinal fluid volume does not have etiological role in the incidence of positional skull deformities

Guillaume Captier [a, e, *], Adrien Galeron [a, b], Gérard Subsol [b], Melissa Solinhac [a, b], Thomas Roujeau [c], Nicolas Leboucq [d], Christian Herlin [a, b]

[a] Department of Plastic and Craniofacial Pediatric Surgery (Head: Guillaume Captier), Lapeyronie University Hospital, Avenue Du Doyen Gaston Giraud, Montpellier, France
[b] Research-Team ICAR, LIRMM CNRS, University of Montpellier, France
[c] Department of Pediatric Neurosurgery, Guy de Chauliac University Hospital, Avenue Augustin Fliche, Montpellier, France
[d] Department of Neuroradiology, Guy de Chauliac University Hospital, Avenue Augustin Fliche, Montpellier, France
[e] EA2415, Epidemiologic Biostastic and Clinical Research Laboratory, University of Montpellier, France

ARTICLE INFO

Article history:
Paper received 19 December 2016
Accepted 6 June 2017
Available online 13 June 2017

Keywords:
3D imaging
Brain
Segmentation
Non-synostotic plagiocephaly
Brachycephaly
Cerebrospinal fluid

ABSTRACT

Background: Positional skull deformities (PSD) are becoming a daily health concern for craniofacial surgeons. Several reports have indicated that cerebrospinal fluid (CSF) space increases on computed tomography (CT) scans of infants suffering from PSD, suggesting a potential causal link. Here, we describe a semi-automatic method to estimate total brain and CSF volumes quantitatively. We tested the potential correlation between total CSF volume and the occurrence of PSD.
Methods: A single-center retrospective study was carried out using 79 CT scans of PSD and 60 CT scans of control subjects. The endocranium was segmented automatically using a three-dimensional deformable surface model, and the brain was segmented using a semi-automatic threshold-based method. Total CSF volume was estimated based on the difference between endocranial and brain volumes.
Results: Automatic segmentation of the endocranium was possible in 75 CT scans. Semi-automatic brain and CSF volume evaluations were performed in 40 CT scans of infants with PSD (18 = occipital plagiocephaly, 11 = fronto-occipital plagiocephaly, and 11 = posterior brachycephaly) and in six control CT scans. Endocranial and total CSF volumes were not significantly different between patients with PSD and controls. The occipital plagiocephaly group had an enlarged brain volume compared with that in patients in the other groups.
Conclusions: Total CSF volume did not change in infants with PSD, and the results do not support a role for volume changes in CSF in the etiology of PSD. Macrocephaly in patients with occipital plagiocephaly may be a specific etiological factor compared with that in other PSDs.

1. Introduction

The incidence of positional skull deformities (PSD) – positional plagiocephalies or positional posterior brachycephalies (Argenta, 2004) – has increased significantly since the American Academy of Pediatrics published sleeping position recommendations to prevent sudden infant death syndrome (Shweikeh et al., 2013). Almost one in two infants at birth (Kane et al., 1996) and one in five babies during the first 2 months of life develop PSD (Flannery et al., 2012). Aside from esthetic concerns, the impacts of PSD on development remain unclear. Some authors have reported that infants with PSD have a higher risk of psychomotor delay, or visual-spatial or perception defects (Miller and Clarren, 2000; Collett et al., 2011, 2012; Gupta et al., 2003; Siatkowski et al., 2005; Panchal et al., 2001); however, improvements are usually seen at 3–4 years of age (Hutchison et al., 2011, 2012). Furthermore, most of the available studies compared a normal distribution of infants with PSD, who frequently present with other risk factors for developmental delay (Weissler et al., 2016).

* Corresponding author. Department of Plastic and Craniofacial Pediatric Surgery, CHU Lapeyronie, Avenue Du Doyen Gaston Giraud, Montpellier, France. Fax: +33 467330500.
E-mail address: c-herlin@chu-montpellier.fr (G. Captier).

http://dx.doi.org/10.1016/j.jcms.2017.06.005
1010-5182/

The exact etiologies of PSDs are unclear; however, cerebrospinal fluid (CSF) volume abnormalities have been suggested as a potential etiology by several authors (Martinez-Lage et al., 2006). Indeed, computed tomography (CT) studies of children with PSD show excess CSF in the subarachnoid periencephalic space (Sawin et al., 1996). Thus, an increase in CSF volume has been implicated as a factor that augments skull compliance and malleability, and promotes the development of PSD. Conversely, the precise role of an enlarged periencephalic space in patients with PSD has not been determined (Martinez-Lage et al., 2006).

Magnetic resonance imaging (MRI) is the reference imaging method for studying brain structure and CSF (Caviness et al., 1999; Courchesne et al., 2000; Kamdar et al., 2009; Pfefferbaum et al., 1994). However, CT is the preferred technique for analyzing the skull and ruling out craniosynostosis (Tomlinson and Breidahl, 2007; Mazzola et al., 2016). Few promising brain segmentation methods have been developed for CT scans (Gupta et al., 2010; Qian et al., 2013). They have mainly been used to detect hemorrhages; however, they have never been used in clinical studies on PSD. Here we describe a simple automatic method for segmenting the endocranium in three dimensions (3D), using a semi-automatic procedure. We used this new method to estimate CSF volume in infants with PSD. The objective was to evaluate CSF volume in patients with PSD compared with that in a normal group. This procedure could also be applied to other pathologies, such as hydrocephalus (Mandell et al., 2015b).

2. Material and methods

2.1. Subjects

A retrospective single-center study was carried out using a CT-scan database in DICOM format collected at our regional university hospital (IDDN 11-300010-000). This database included anonymized CT scans of 79 infants with PSD, born between 2002 and 2013. After 2007, CT scans were prescribed only when clinical features were not conclusive of PSD (Tomlinson and Breidahl, 2007).

The patients' clinical data were partially screened in a previous study (Captier et al., 2011). The exclusion criterion was strong hypotonia related to major development abnormalities included or not included in a syndrome framework. The markers used were holding the head, seated holding, spontaneous reversal in bed, holding standing supported, walking with support then without support, climbing stairs, running, jumping, and babbling. PSD was differentiated by age when one- and two-word sentences appeared.

CT scans of children with PSD were performed under general anesthesia to generate a 3D reconstruction of the skull. Images were acquired using a Siemens CT scanner (Siemens Healthcare, Erlangen, Germany) with a 0.5-mm slice width (512 × 512 pixels).

Based on an analysis of 79 CT scans, positional deformities were categorized, according to the classification by Captier et al. (2011), as follows: occipital plagiocephaly (Demiri et al., 2013) ($n = 28$; mean age, 8.95 months; range, 4–16 months; sex ratio, 1.33), fronto-occipital plagiocephaly (FOP) ($n = 33$; mean age, 8.28 months; range, 4–23 months; sex ratio, 1.35), and posterior brachycephaly (PB) ($n = 18$; mean age, 8.06 months; range, 5–21 months; sex ratio, 1.57).

A group of 60 CT scans of children (mean age, 9.57 months; range, 1–23 months; sex ratio, 1.5) without PSD and whose pathology did not affect skull shape were selected as controls (head trauma without any anatomical abnormality).

The quality of the native CT image was judged visually by an imaging expert (AG), and only images with sharp differentiation between the brain, CSF, and skull were used for the study.

2.2. 3D segmentation of skull and endocranium

The skull and endocranium (inner surface of the skull) were segmented into a 3D surface mesh using the CT scans. The skull was segmented semi-automatically using Myrian software (Intrasense, Montpellier, France) and exported into Endex software (http://liris.cnrs.fr/gilles.gesquiere/wiki/doku.php?id=endex) for automatic segmentation of the endocranium. This segmentation method is based on a 3D deformable surface (Subsol et al., 2010). By summing the volumes of all the cones formed by faces of the 3D surface mesh with respect to the origin, it was easy to compute the volumes of the 3D skull and endocranium meshes.

2.3. 3D brain segmentation

The brain segmentation method was based on intensity thresholding (Mikheev et al., 2008) and was implemented using Fiji software (http://fiji.sc/Fiji). First, an intensity threshold was adjusted to visually separate brain structures (in white in Fig. 1, right panel) from the remainder of the 3D image.

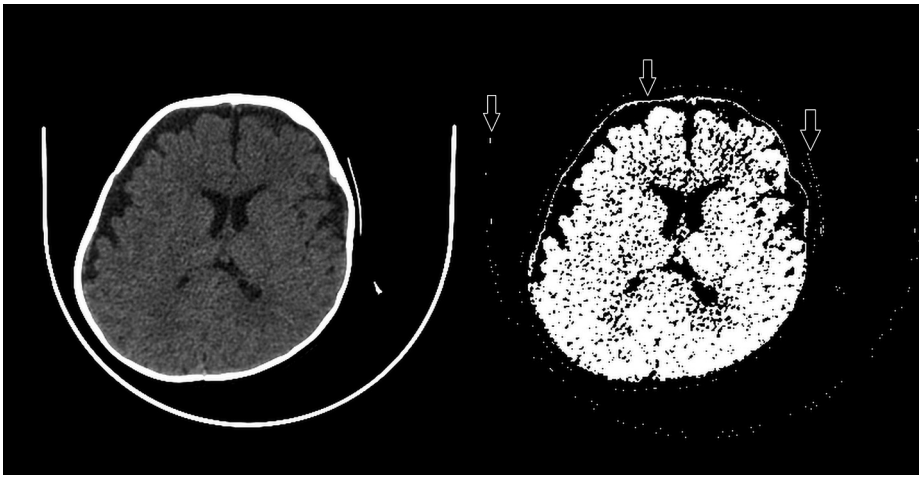

Fig. 1. Computed tomography (CT) scan of an infant with fronto-occipital plagiocephaly (FOP) before (left) and after (right) manual thresholding. Some exocranial structures are included (arrows), and 'holes' (black) are visible within the encephalon (white).

Nevertheless, some connections between the structure to be segmented (brain) and some extra-encephalic structures (in particular the cranial layer) were still present. To remove them, we 'shaved' them off using a 3D erosion step (Fig. 2A). This resulted in several 3D white regions in the image that we could identify. We then selected the largest one, which corresponded to the brain (Fig. 2B). A 3D dilation of this component was then applied to compensate for the erosion (Fig. 2C). Visible holes in the brain were caused by voxels with an intensity below that used for thresholding (Fig. 2D). These holes, which probably correspond to intracerebral vascular structures, were filled by 3D dilation, followed by a 3D erosion step to form the initial shape of the brain, except without the holes.

Finally, the resulting binary 3D segmented image was transformed into a 3D surface mesh using the classical marching cubes algorithm. We then directly computed the volume of the brain 3D mesh. By subtracting the endocranium and the brain volume, we estimated the total CSF volume (subsrachnoid spaces and ventricles).

2.4. Study parameters

Brain and endocranial volumes were measured from the 3D surface mesh obtained after 3D segmentation. The volume distribution was then assessed as a function of age (0–2 years of age) and compared among the three PSD groups and controls.

Total CSF volume was calculated by subtracting brain volume from endocranial volume. Therefore, total CSF volume included the fluid contained in the subarachnoid spaces, ventricles, and the vascular compartment of the venous sinuses.

2.5. Statistical analysis

Based on the hypothesis of a normal distribution of volume variables for the population, Dunnett's test was used to compare multiple variables in the three experimental groups. The statistical analysis was performed using IBM SPSS Statistics 22 (IBM Corp., Armonk, NY, USA).

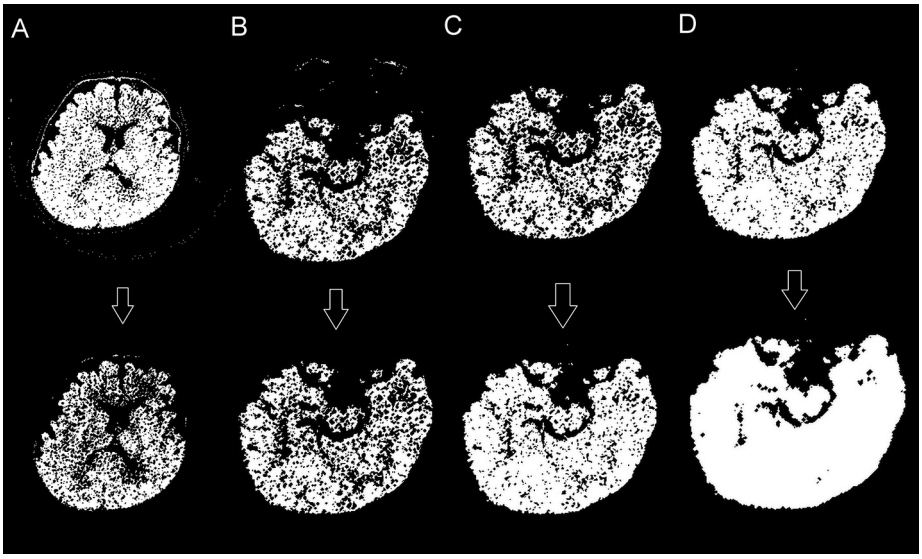

Fig. 2. After manual thresholding (Fig. 1), the three-dimensional brain segmentation method included: A) 3D erosion of the image to cut the bridges between the structure to be segmented (brain) and the remainder of the image (top image before and bottom image after the procedure); B) selection of the main component (top image before and bottom image after); C) 3D dilation of the image (top image before and bottom image after); and D) hole filling by 3D dilation (top panel) followed by 3D erosion (bottom panel).

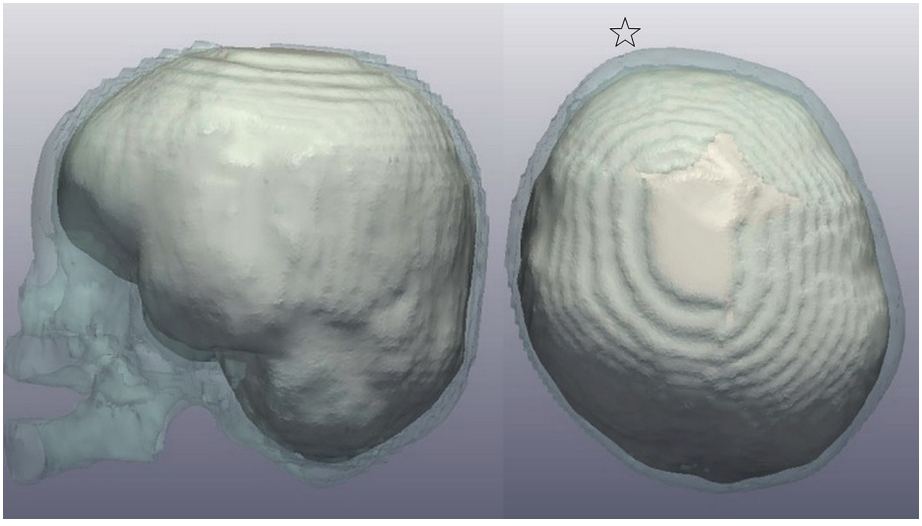

Fig. 3. Three-dimensional segmentation of the skull and endocranium of an infant with fronto-occipital plagiocephaly (FOP) (star indicates frontal bulging).

3. Results

3.1. 3D endocranial segmentation

The endocranium was automatically segmented in 64 children with PSD (24 OP, 24 FOP, and 16 PB) (mean age, 9.1 months; range, 1–23 months; sex ratio, 1.46) and 11 controls (mean age, 7.3 months; range, 1–23 months; sex ratio, 1.2). The 3D surface mesh allowed us to analyze the effect of PSD on the endocranium and to estimate endocranial volume (Fig. 3). The brain impressions on the endocranium, particularly in the occipital region, indicated that 3D segmentation produced good results. The 3D mesh allowed highlighting of the structural differences between the endocranium of the controls and that of the infants with PSD. Specifically, the endocranium of infants with PB was wider and flattened, whereas it was unilaterally flattened in patients with OP, and a frontal bulge was present in infants with FOP (arrows in Fig. 3).

3.2. 3D brain segmentation

Visual differentiation of the skull, brain, and peri-encephalic spaces was sufficient in 40 patients with PSD (18 OP, 11 FOP, and 11 PB) (mean age, 8.5 months; range, 3–23 months; sex ratio, 1.22) and six controls (mean age, 10 months; range, 4–23 months; sex ratio, 1). The 3D brain segmentation method allowed correct visualization of the two hemispheres, sulci, and gyri (Fig. 4). In some cases, a partial volume effect due to limited CT spatial resolution was observed, making it difficult to visualize the gyri, particularly the area where the cortex was very close to the skull, such as the occipital region. 3D brain segmentation also highlighted the presence and severity of brain cortical deformities in the three PSD types.

3.3. Volumetric analysis

Endocranial volumes in infants with FOP, OP, and PB, as well as in the controls, were comparable despite variability in the data ($p = 0.42$, $p = 0.30$, and $p = 0.14$, respectively; Fig. 5). On the other hand, infants with OP had a slightly larger brain volume than the controls ($p = 0.04$; Fig. 6). No difference was observed between the control and FOP groups ($p = 0.44$), and between the control and PB groups ($p = 0.19$). Total CSF volumes in the FOP, OP, and PB groups did not differ compared with those in the control group ($p = 0.84$, $p = 0.49$, and $p = 0.49$, respectively; Fig. 7).

4. Discussion

The semi-automatic 3D brain segmentation method that we developed is efficient and simple to implement. This innovative method allowed us to analyze and quantify endocranial and brain volumes, and to estimate total CSF volume from CT scans of infants with PSD. This method can be implemented using existing 3D image treatment tools, such as Fiji or Matlab® (Mathworks, Natick, MA, USA), and requires only a few seconds for calculation. Application by clinicians could allow the study of other pathologies that require CT examinations involving CSF and brain volumes, such as hydrocephalus.

Very limited data have been published on brain and CSF volumes in patients with PSD, and no proper 3D volumetric studies have been performed. Our results suggest that total CSF volume did not increase in patients with PSD compared with that in controls, and could not be considered an etiological factor. This is in contrast to the findings reported by Sawin et al. (1996) and Martinez-Lage et al. (2006). Sawin et al. (1996) manually quantified the volumes of some localized peri-encephalic spaces in two dimensions, but not total CSF volume (subarachnoid spaces and ventricles). They found that periencephalic space volume increased in infants with OP, whereas this was only rarely the case for ventricular volume. Larger periencephalic space volumes in patients with PSD ($n = 23$) were also found by Martinez-Lage et al. (2006), particularly at the levels of the frontal region and lateral sulcus. No quantitative data were reported. The difference from our findings could be explained by the fact that our method includes the entire subarachnoid space and does not distinguish between subarachnoid space, ventricular, and CSF volumes.

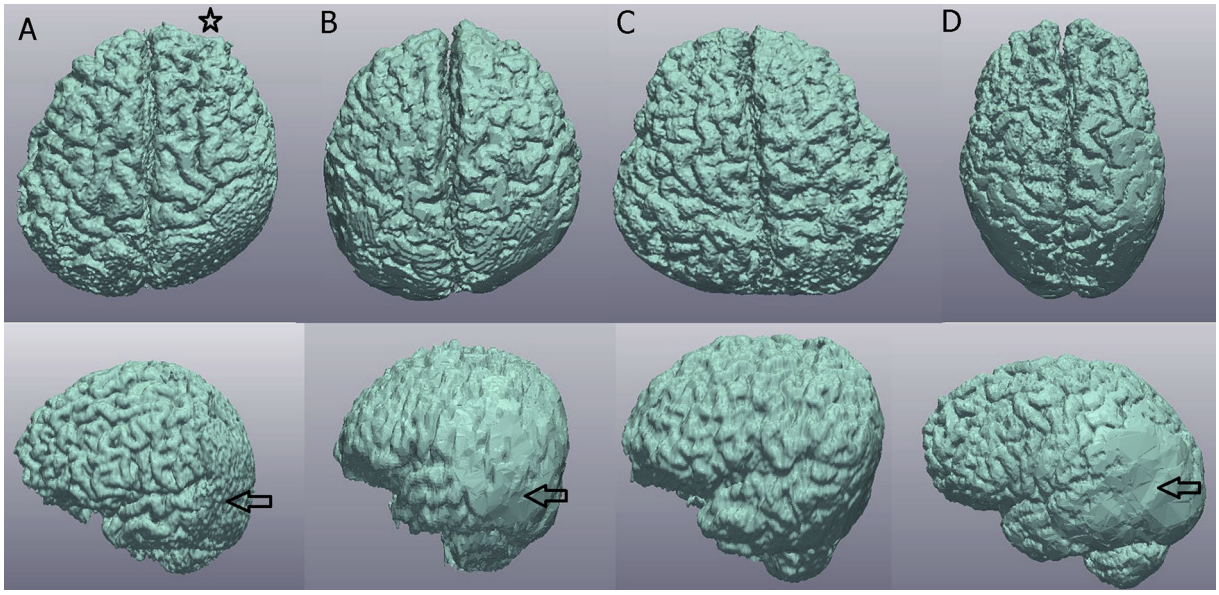

Fig. 4. Three-dimensional brain visualization after 3D segmentation and surface reconstruction: A) example of fronto-occipital plagiocephaly (FOP); B) example of occipital plagiocephaly (1); C) example of posterior brachycephaly (PB); and D) control. Top panels, rear view; bottom panels, lateral view. A partial volume effect occasionally produced poorer visualization of the gyri, such as in the occipital region (arrows). Note the presence of the encephalon deformity in the three positional skull deformity (PSD) types: frontal bossing (star) on the same side of occipital flattening in A), unilateral occipital flattening in B), and bilateral, more-or-less symmetric occipital flattening in C).

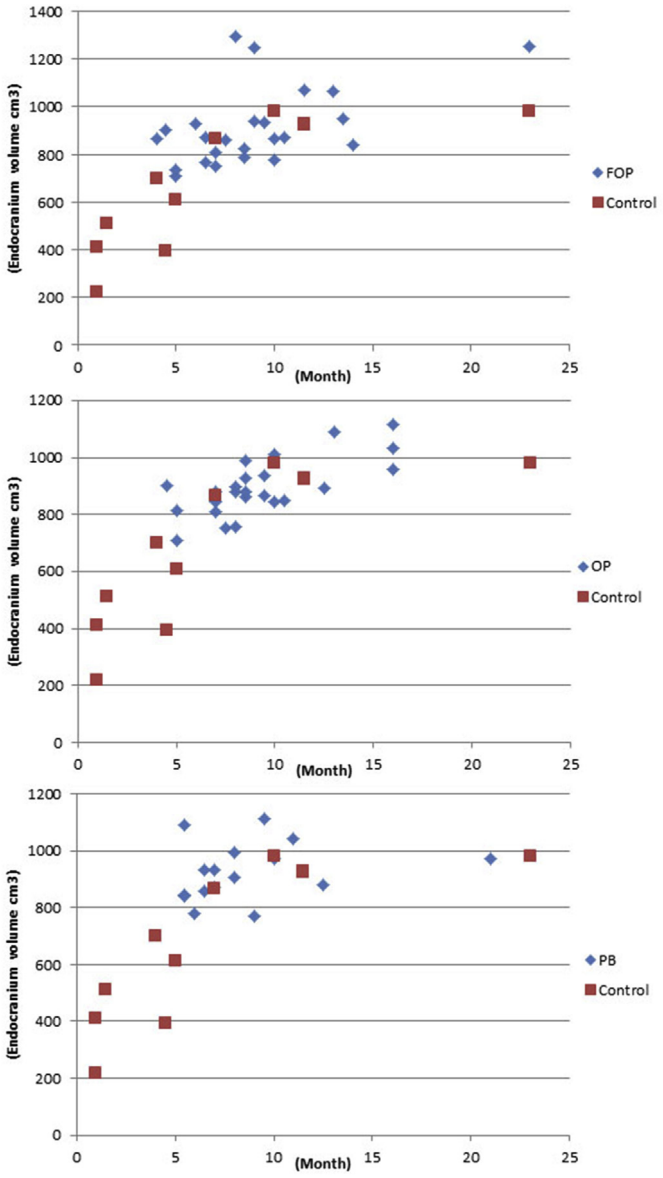

Fig. 5. Distribution of the endocranial volume data (in cm^3) for infants with positional skull deformities (PSD) (blue) and controls as a function of their age (in months) – 24 occipital plagiocephaly (OP), 24 fronto-occipital plagiocephaly (FOP), 16 posterior brachycephaly (PB), and 11 controls.

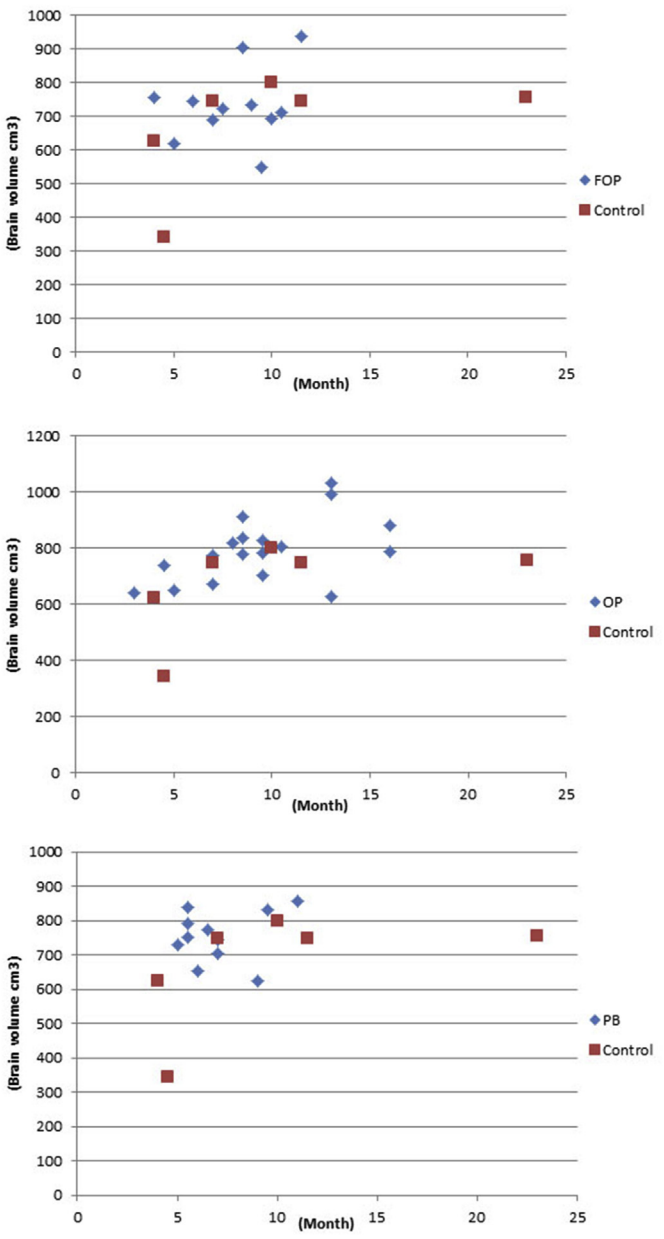

Fig. 6. Distribution of the brain volume data (cm^3) for infants with positional skull deformities (PSD) (blue) and controls as a function of their age (in months) – 18 occipital plagiocephaly (OP), 11 fronto-occipital plagiocephaly (FOP), 11 posterior brachycephaly (PB), and six controls.

Our endocranial volume results are comparable to previously published MRI images in infants with dry skull (Courchesne et al., 2000; Coqueugniot and Hublin, 2012). Finally, as in our study, the brain volume estimates reported by Collett et al. (2012) did not highlight any difference between infants with PSD and controls.

Visualizing the brains of infants with PSD in 3D highlights that skull and endocranial deformities have an effect on brain cortical morphology. For example, the brains of infants with PB show the same posterior flattening as the endocranium and the external surface of the skull. Some authors have suggested that such cerebral compression or deformation (particularly in the occipital region) could be a cause of the psychomotor abnormalities observed in infants with PSD (Siatkowski et al., 2005; Panchal et al., 2001).

In our study, infants with OP had larger brain volumes than controls. In addition, some authors have reported that macrocephaly can affect motor development (Biran-Gol et al., 2010; Smith et al., 1984). This finding should be confirmed by larger studies and could support the hypothesis that developmental delay plays a role in PSD, particularly in OP etiopathogeny, and not the contrary as reported by Weissler et al. in their recent literature review and analysis (Weissler et al., 2016).

Three-dimensional brain segmentation has been accomplished previously using MRI images (Kamdar et al., 2009; Pfefferbaum et al., 1994), but very rarely using CT scans (Muschelli et al., 2015). Gupta et al. (2010) developed a segmentation algorithm for CSF and white and gray matter based on 70 unenhanced CT scans, but they did not propose 3D visualization or a volume calculation. On the other hand, Kemmling et al. (2012) suggested using probabilistic tissue maps of these different structures derived from 600 MRIs. These maps were adapted for segmenting CT scans using a non-rigid adjustment algorithm. The authors described some potential applications but no clinical study. Mandell et al. (2015a) proposed

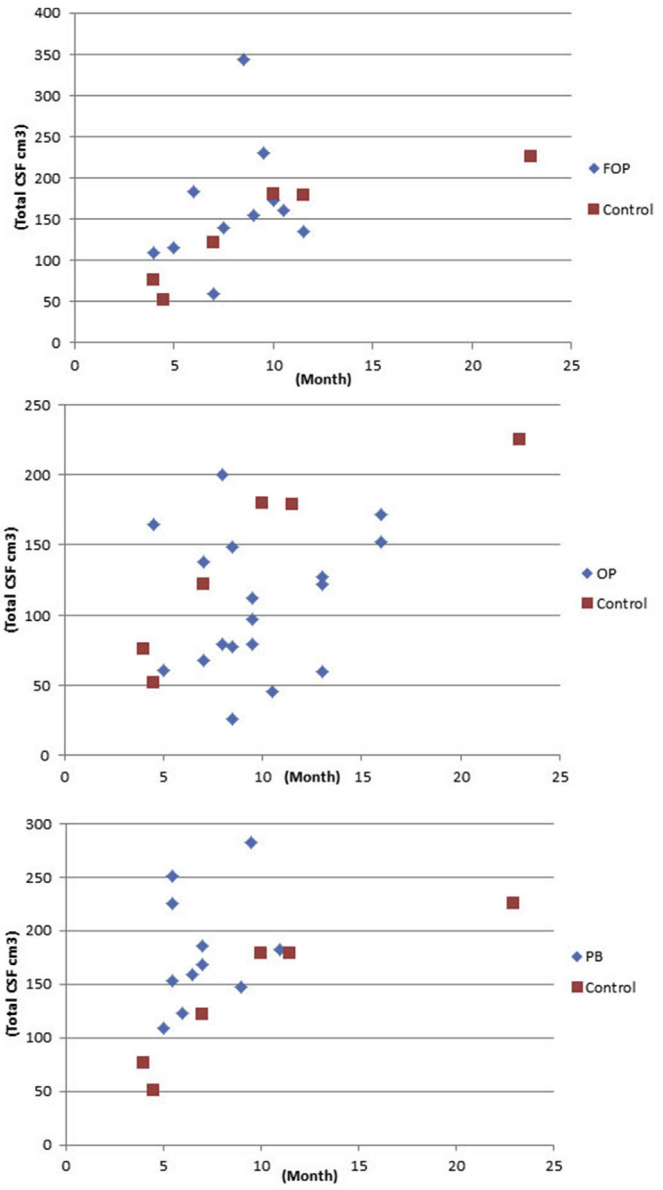

Fig. 7. Total cerebrospinal fluid (CSF) volume in infants with positional skull deformities (PSD) (blue) and controls as a function of their age (in months) – 18 occipital plagiocephaly (OP), 11 fronto-occipital plagiocephaly (FOP), 11 posterior brachycephaly (PB), and six controls.

adapting the particle filter segmentation algorithm used on MRI for CT scans of pediatric hydrocephalus.

Our semi-automatic method for 3D brain segmentation based on a CT scan is simple and efficient, but the major problem with CT scans is the quality of the native image. Indeed, in routine examinations without pre-established acquisition protocol, the intensity differentiation between brain structures and CSF is often too limited and does not allow the 3D brain to be segmented correctly. This explains the strict selection of suitable CT scans. The resulting low number of control CT scans represents a strong limitation of our study, and should be increased to draw definitive conclusions. A way to optimize the brain segmentation algorithm is to use this method on every CT scan independently of the native image. Another limitation of our study concerns the differences between the median ages of the groups, although the initial distributions were identical.

It might be useful to estimate the CSF present in the ventricles and in the subarachnoid spaces separately when quantifying CSF volume in each type of PSD. This would allow clinicians to refine their diagnosis and substantiate physiopathological hypotheses. In our method, CSF volume is estimated based on the difference between the endocranial and brain volumes. One limitation of this method is that CSF and dural venous sinus volumes must be combined, so further study is necessary to determine how to perform autonomous segmentation using these two different compartments. Qian et al. (2013) proposed a direct CSF segmentation method using CT scans. It would be interesting to compare their direct method with our indirect procedure for quantifying CSF volume.

5. Conclusions

We have proposed a simple, efficient, and reliable 3D method for segmenting intracranial components semi-automatically. This new method enabled us to test the hypothesis of the mechanical participation of the CSF in PSD. Total CSF volume in infants with PSD did not differ from that in controls, so a role for changes in CSF volume in the etiology of PSD was not supported. Macrocephaly in the population with BP may be a specific etiological factor compared with the other PSD.

Author's contribution

GC: Concept and design of the study, data acquisition, statistical analysis and interpretation.
AG: Data acquisition, statistical analysis and interpretation.
GS: Concept and design of the study, data interpretation.
MS: Critical revision and approval of final manuscript to submit.
TR: Critical revision and approval of final manuscript to submit.
NL: Data acquisition, data interpretation.
CH: Concept and design of the study, data acquisition, statistical analysis and interpretation.

Disclosures and funding

Part of results of this work was presented as a poster at the French research meeting Journées Ouvertes en Biologie, Informatique & Mathématiques 2013, Toulouse, France.

None of the authors has a financial interest in any of the products, devices, or drugs mentioned in this manuscript.

Conflict of interest

Authors declare no potential conflicts of interest.

Acknowledgments

We thank Ostéobio (Cachan, France) for funding the graduate training of Adrien Galeron and Melissa Solinhac during their Master STIC-Santé BCD specialty at the University of Montpellier, France. We also thank Dr. Paul Landais for the statistical analysis and Dr. Magali Sagintah for helping with the CT scans.

References

Argenta L: Clinical classification of positional plagiocephaly. J Craniofac Surg 15: 368–372, 2004
Biran-Gol Y, Malinger G, Cohen H, Davidovitch M, Lev D, Lerman-Sagie T, et al: Developmental outcome of isolated fetal macrocephaly. Ultrasound Obstet Gynecol 36: 147–153, 2010
Caviness Jr VS, Lange NT, Makris N, Herbert MR, Kennedy DN: MRI-based brain volumetrics: emergence of a developmental brain science. Brain Dev 21: 289–295, 1999
Captier G, Dessauge D, Picot MC, Bigorre M, Gossard C, El Ammar J, et al: Classification and pathogenic models of unintentional postural cranial deformities in infants: plagiocephalies and brachycephalies. J Craniofac Surg 22: 33–41, 2011
Collett BR, Starr JR, Kartin D, Heike CL, Berg J, Cunningham ML, et al: Development in toddlers with and without deformational plagiocephaly. Arch Pediatr Adolesc Med 165: 653–658, 2011

Collett BR, Aylward EH, Berg J, Davidoff C, Norden J, Cunningham ML, et al: Brain volume and shape in infants with deformational plagiocephaly. Childs Nerv Syst 28: 1083–1090, 2012
Coqueugniot H, Hublin JJ: Age-related changes of digital endocranial volume during human ontogeny: results from an osteological reference collection. Am J Phys Anthropol 147: 312–318, 2012
Courchesne E, Chisum HJ, Townsend J, Cowles A, Covington J, Egaas B, et al: Normal brain development and aging: quantitative analysis at in vivo MR imaging in healthy volunteers. Radiology 216: 672–682, 2000
Demiri E, Papaconstantinou A, Dionyssiou D, Dionyssopoulos A, Kaidoglou K, Efstratiou I: Reconstruction of skin avulsion injuries of the upper extremity with Integra® dermal regeneration template and skin grafts in a single-stage procedure. Arch Orthop Trauma Surg 133: 1521–1526, 2013
Flannery AB, Looman WS, Kemper K: Evidence-based care of the child with deformational plagiocephaly, part II: management. J Pediatr Health Care 26: 320–331, 2012
Gupta PC, Foster J, Crowe S, Papay FA, Luciano M, Traboulsi EI: Ophthalmologic findings in patients with nonsyndromic plagiocephaly. J Craniofac Surg 14: 529–532, 2003
Gupta V, Ambrosius W, Qian G, Blazejewska A, Kazmierski R, Urbanik A, et al: Automatic segmentation of cerebrospinal fluid, white and gray matter in unenhanced computed tomography images. Acad Radiol 17: 1350–1358, 2010
Hutchison BL, Stewart AW, de Chalain T, Mitchell EA: Serial developmental assessments in infants with deformational plagiocephaly. J Paediatr Child Health 48: 274–278, 2012
Hutchison BL, Stewart AW, Mitchell EA: Deformational plagiocephaly: a follow-up of head shape, parental concern and neurodevelopment at ages 3 and 4 years. Arch Dis Child 96: 85–90, 2011
Kamdar MR, Gomez RA, Ascherman JA: Intracranial volumes in a large series of healthy children. Plast Reconstr Surg 124: 2072–2075, 2009
Kane AA, Mitchell LE, Craven KP, Marsh JL: Observations on a recent increase in plagiocephaly without synostosis. Pediatrics 97: 877–885, 1996
Kemmling A, Wersching H, Berger K, Knecht S, Groden C, Nolte I: Decomposing the Hounsfield unit: probabilistic segmentation of brain tissue in computed tomography. Clin Neuroradiol 22: 79–91, 2012
Mandell JG, Langelaan JW, Webb AG, Schiff SJ: Volumetric brain analysis in neurosurgery: part 1. Particle filter segmentation of brain and cerebrospinal fluid growth dynamics from MRI and CT images. J Neurosurg Pediatr 15: 113–124, 2015a
Mandell JG, Kulkarni AV, Warf BC, Schiff SJ: Volumetric brain analysis in neurosurgery: Part 2. Brain and CSF volumes discriminate neurocognitive outcomes in hydrocephalus. J Neurosurg Pediatr 15: 125–132, 2015b
Martinez-Lage JF, Ruiz-Espejo AM, Gilabert A, Perez-Espejo MA, Guillen-Navarro E: Positional skull deformities in children: skull deformation without synostosis. Childs Nerv Syst 22: 368–374, 2006
Mazzola C, Baird LC, Bauer DF, Beier A, Durham S, Klimo Jr P, et al: Congress of neurological surgeons systematic review and evidence-Based guideline for the diagnosis of patients with positional plagiocephaly: the role of imaging. Neurosurgery 79: 625–626, 2016
Mikheev A, Nevsky G, Govindan S, Grossman R, Rusinek H: Fully automatic segmentation of the brain from T1-weighted MRI using bridge burner algorithm. J Magn Reson Imaging 27: 1235–1241, 2008
Miller RI, Clarren SK: Long-term developmental outcomes in patients with deformational plagiocephaly. Pediatrics 105: 26, 2000
Muschelli J, Ullman NL, Mould WA, Vespa P, Hanley DF, Crainiceanu CM: Validated automatic brain extraction of head CT images. Neuroimage 114: 379–385, 2015
Panchal J, Amirsheybani H, Gurwitch R, Cook V, Francel P, Neas B, et al: Neurodevelopment in children with single-suture craniosynostosis and plagiocephaly without synostosis. Plast Reconstr Surg 108: 1492–1498, 2001
Pfefferbaum A, Mathalon DH, Sullivan EV, Rawles JM, Zipursky RB, Lim KO: A quantitative magnetic resonance imaging study of changes in brain morphology from infancy to late adulthood. Arch Neurol 51: 874–887, 1994
Qian X, Wang J, Guo S, Li Q: An active contour model for medical image segmentation with application to brain CT image. Med Phys 40: 1911, 2013
Sawin PD, Muhonen MG, Menezes AH: Quantitative analysis of cerebrospinal fluid spaces in children with occipital plagiocephaly. J Neurosurg 85: 428–434, 1996
Shweikeh F, Nuño M, Danielpour M, Krieger MD, Drazin D: Positional plagiocephaly: an analysis of the literature on the effectiveness of current guidelines. Neurosurg Focus 35: E1, 2013
Siatkowski RM, Fortney AC, Nazir SA, Cannon SL, Panchal J, Francel P, et al: Visual field defects in deformational posterior plagiocephaly. J AAPOS 9: 274–278, 2005
Smith RD, Ashley J, Hardesty RA, Tulley R, Hewitt J: Macrocephaly and minor congenital anomalies in children with learning problems. J Dev Behav Pediatr 5: 231–236, 1984
Subsol G, Gesquière G, Braga J, Thackeray F: 3D automatic methods to segment 'virtual' endocasts: state of the art and future directions. Am J Phys Anthropol 141: 226–227, 2010
Tomlinson JK, Breidahl AF: Anterior fontanelle morphology in unilateral coronal synostosis: a clear clinical (nonradiographic) sign for the diagnosis of frontal plagiocephaly. Plast Reconstr Surg 119: 1882–1888, 2007
Weissler EH, Sherif RD, Taub PJ: An evidence-based approach to nonsynostotic plagiocephaly. Plast Reconstruct Surg 138: 682–689, 2016